Ultrasonics Sonochemistry 115 (2025) 107302

Contents lists available at ScienceDirect

Ultrasonics Sonochemistry

journal homepage: www.elsevier.com/locate/ultson

Ultrasound-assisted preparation of shikonin-loaded emulsions for the treatment of bacterial infections

Xiaomiao Cui [a], Zhiliang Gao [a], Xinxin Han [a], Qun Yu [a], Vitoria H. Cauduro [b], Erico M.M. Flores [b], Muthupandian Ashokkumar [c], Xiaoyong Qiu [a,*], Jiwei Cui [a,d,*]

[a] Key Laboratory of Colloid and Interface Chemistry of the Ministry of Education, School of Chemistry and Chemical Engineering, Shandong University, Jinan, Shandong 250100, China
[b] Department of Chemistry, Federal University of Santa Maria, Santa Maria 97105-900 RS, Brazil
[c] School of Chemistry, The University of Melbourne, Parkville, VIC 3010, Australia
[d] Shandong Key Laboratory of Targeted Drug Delivery and Advanced Pharmaceutics, Shandong University, Jinan, Shandong 250100, China

ARTICLE INFO

Keywords:
Bacterial biofilm
α-Amylase
Polyphenol
Ultrasound
Emulsion
Wound healing

ABSTRACT

Bacteria can encapsulate themselves in a self-generated matrix of hydrated extracellular polymeric substances such as polysaccharides, proteins, and nucleic acids, thereby forming bacterial biofilm infections. These biofilms are drug resistant and will diminish the efficacy of antimicrobial agents, rendering treatment of such infections challenging. Herein, an innovative strategy is proposed to synergistically degrade bacterial biofilms and eradicate the entrapped bacteria through integrating α-amylase (α-Amy), shikonin (SK) and epigallocatechin gallate (EGCG) within an emulsion. The natural protein α-Amy is deployed to enzymatically hydrolyze the polysaccharide of biofilms. Due to the amphipilic properties of α-Amy and the cross-linking capability of EGCG, the formed α-Amy/SK@EGCG emulsion possess high stability. SK was encapsulated within the emulsion through ultrasound-assisted assembly, targeting to treat bacterial infection after biofilm degradation. *In vitro* and *in vivo* experiments demonstrate that the polyphenol-protein stabilized emulsion loaded with antibacterial SK achieves profound penetration into the biofilms due to the extracellular polysaccharide hydrolysis mediated by α-Amy. As a result, the α-Amy/SK@EGCG emulsion can significantly alleviate inflammation symptoms and accelerate the healing process of biofilm-infected wounds. This study provides a promising therapeutic strategy for the development of novel materials aimed for the enhanced treatment of bacterial biofilm infections.

1. Introduction

The antibiotic resistant properties of bacterial biofilms have posed a significant threat to public health [1]. These biofilms assembled by bacteria communities adhere to the surface of wound tissues, making them hardly to be treated. The bacteria are encased in a self-generated matrix of hydrated extracellular polymeric substances (EPS), which are comprised of polysaccharides, DNA, proteins, and lipids, accounting for more than 90 % of the biofilm's dry weight [2]. These biopolymers in EPS would form a three-dimensional network to envelop the bacteria and act as a protective barrier [3]. This barrier not only impedes the penetration of antimicrobial agents, but also increases biofilm resistance to antibiotics by up to 1000-fold compared to the planktonic bacteria. Various wounds, such as surgical wounds, burn wounds, diabetic foot and mouth ulcers, offer a nutrient-rich environment that is conducive to biofilm formation and growth, thereby increasing the risk of biofilm-associated infections [4]. The presence of biofilm would significantly impede wound healing, leading to chronic infections and even life-threatening conditions [5]. Consequently, bacterial biofilms with high drug resistance have emerged as a critical public health challenge in the 21st century [6–9]. In this sense, the development of effective strategies for the degradation of bacterial EPS is paramount for optimal drug delivery [4,10,11].

The primary methodologies for biofilm degradation are physical removal and chemical dissolution. Physical removal needs to peel the biofilm off from the wound by mechanical force, which requires repeated debridement and carries the risk of wound recurrence due to residual biofilm [12]. In contrast, chemical dissolution typically

* Corresponding authors at: Key Laboratory of Colloid and Interface Chemistry of the Ministry of Education, School of Chemistry and Chemical Engineering, Shandong University, Jinan, Shandong 250100, China.
E-mail addresses: xyqiu@sdu.edu.cn (X. Qiu), jwcui@sdu.edu.cn (J. Cui).

https://doi.org/10.1016/j.ultsonch.2025.107302
Received 5 January 2025; Received in revised form 26 February 2025; Accepted 4 March 2025
Available online 4 March 2025

employs nanomaterials (e.g. nanoparticles, polymers and liposomes) to encapsulate antibiotics and degrade biofilms [12–16]. However, the presence of the EPS matrix restrict the penetration of these nanomedicines, leading to unsatisfactory therapeutic effect [17]. The therapeutic effect can be improved by applying external conditions, such as photothermal therapy, electrical stimulation, and ultrasound, but they inevitably cause non-specific damage to healthy tissue [18–21]. A promising therapeutic strategy to counteract bacterial biofilms is targeting the disruption of key EPS components to increase the susceptibility of biofilms to antibiotics [9]. In this regard, the α-amylase (α-Amy) enzyme has demonstrated potential as a high-performance biofilm degradation agent, which can effectively hydrolyze exopolysaccharides that contains α-1,4-glucosidic bonds to oligosaccharides [22,23]. Research by Tzanko et al. has showed that *α*-Amy can effectively break down polysaccharide component of EPS, disrupting the biofilms of *S. aureus* and *P. aeruginosa*, and subsequently enhancing the effectiveness of antibiotics [24,25].

Over the decades, antibiotics have played vital role in eliminating infectious bacterial biofilms. However, the escalating usage of antibiotics, together with the employment of inappropriate antibiotics, which may lead to the spread of antibiotic-resistant bacteria, have already posed a significant threat to the public health [26–28]. In this sense, the development of alternative treatments for bacterial biofilm infection that do not involve the use of antibiotic is of great interest. Shikonin (SK), extracted from the roots of plants in the Boraginaceae family (such as lithospermum erythrorhizon), is a purplish-red natural molecule derived from naphthoquinone. Its derivatives and nano-formulations have significant bioactive properties, such as antioxidant, anti-inflammatory and antibacterial activities. Hence, SK has been widely applied in the treatment of several health issues, including breast cancer, colon cancer, injuries (such as burns and cuts), and others [29,30]. Due to the excellent antibacterial activity against Gram-positive bacteria (such as *S. aureus*), SK emerges as a promising alternative therapy for bacteria-infected burn wounds [31,32]. In this context, SK works by modulating the bacteria adhesion to peptidoglycan and compromising the integrity of cell membranes. However, the use of SK in biomedical field is constrained by certain critical challenges, such as the limited water solubility and low stability [32]. Consequently, it is necessary to develop drug delivery systems that can enhance the bioactivity, stability, and bioavailability of SK. To address these limitations, oil-in-water (O/W) emulsions have been applied for hydrophobic drugs delivery [33,34]. The emulsion serves as a protective vehicle for drugs encapsulated within its oil phase, protecting them from the harsh external environment and imparting a sustained-release effect, thereby the bioavailability of the encapsulated drug was enhanced [35–37]. Moreover, natural amphiphilic proteins can be utilized as emulsifiers in place of traditional surfactants, providing stabilization to O/W emulsions [38,39]. These proteins exhibit several distinct advantages, including environment friendly, biodegradable, minimal toxic to human body, and biocompatible [40,41].

Herein, the SK-loaded emulsions stabilized by *α*-Amy and epigallocatechin gallate (EGCG) (α-Amy/SK@EGCG) were reported through sono-assembly, aiming for the degradation of bacterial biofilms and eradication of bacteria in wound infections. Compared to traditional methods (mechanical agitation), the emulsions prepared by ultrasound have a smaller and more homogeneous particle size distribution due to the strong shear force generated during the ultrasonication process in a short time. It can also improve the solubility and adsorption efficiency of surfactants at the interface [42]. The emulsification process was facilitated by employing *α*-Amy solution as the continuous phase, and SK dissolved in isopropyl myristate (IPM) serving as the dispersed phase. The rationale for selecting the specific oil phase is that, IPM is an ester-based oil that is widely utilized in pharmaceutical and cosmetic formulations. Characterized by low viscosity and high spreadability, IPM facilitates the uniform distribution of active ingredients (e.g. SK) within formulations. Furthermore, IPM is known for its remarkable skin penetration enhancement properties, which has the potential for improving transdermal delivery of emulsions into skin tissues [43,44]. The α-Amy/SK@EGCG emulsion was prepared through ultrasonication and stabilized by a polyphenol (*viz.* EGCG) that cross-linked with α-Amy at the oil–water interface. The general procedures for emulsification and wound treatment are shown in Scheme 1. The enhanced emulsion stability of α-Amy/SK@EGCG was attributed to non-covalent bonding interactions (including hydrogen bonding, hydrophobic and electrostatic interactions) between polyphenols and proteins. The α-Amy could effectively enhance drug penetration permeation within the wound environment. EGCG not only stabilized the protein–polyphenol emulsion through its cross-linking with α-Amy, but also exerts antimicrobial activity which can play synergistic effect with SK during the treatment. This study demonstrates the effectiveness of polyphenol-protein emulsion in biofilm degradation and drug penetration, which is crucial for improving bacterial inactivation and promoting wound healing.

2. Results and discussion

2.1. Preparation and characterization of α-Amy/SK@EGCG emulsions

Protein-polyphenol stabilized emulsions were prepared by ultrasound-assisted emulsification. An α-Amy solution in PBS was used as the emulsifier, and a SK solution in IPM was used as the oil phase. The mixture was emulsified with an ultrasound probe at 150 W. The interaction between ultrasonic waves and bubbles in a liquid generates acoustic cavitation. When acoustic cavitation bubbles collapse, strong shear forces are generated, which are responsible for the emulsification process. The ultrasonically generated emulsion was further homogenized by using a high-pressure homogenizer to obtain droplets with uniform size. Subsequently, the polyphenol EGCG was introduced to cross-link with the protein at the droplet surface, thereby enhancing the stability of the emulsion. Optical microscopy (Fig. 1a) and TEM (Fig. 1b) images showed the good dispersibility of the droplets, which proved the successful formation of emulsions.

The hydrodynamic diameter of emulsion droplets was ~310 nm (Fig. 1c) with a ζ-potential of −21.0 ± 1.0 mV (Fig. S1). The zeta-potential of the emulsions indicates moderate electrostatic stabilization of the α-Amy/SK@EGCG emulsion. Even though the zeta potential has less effect on the penetration of our emulsion on bacterial biofilms, the nanoscale emulsion facilitates its penetration into the biofilm and disrupts the bacterial biofilm through an enzyme-catalyzed reaction. The size of the α-Amy/SK@EGCG emulsion could be tuned from 331.2 nm to 2147.7 nm by adjusting the ultrasonication time (Fig. S2). In addition, the ultrasonication time can also be used to tune capsule size from 947.2 nm to 331.2 nm (Fig. S3). In order to improve the bioavailability of the emulsion, we therefore chose a power of 150 W and a sonication time of 2 min for the preparation of the emulsion. In order to investigate the crosslinking of α-Amy/SK@EGCG, FTIR spectra of the EGCG powder, α-Amy powder, and α-Amy/SK@EGCG powder were examined (Fig. S4). The broad characteristic peak of α-Amy at 3406 cm^{-1} was assigned to the N–H stretching vibrations. The peak at 2926 cm^{-1} was correspond to the C–H stretching vibration. The peaks at 1530 cm^{-1} were attributed to the carboxy group and carboxymethyl group. The vibration modes found at 1650 cm^{-1} and the region between 1530 cm^{-1} correspond to amides I and II. For EGCG, the broad band at 3356 cm^{-1} and the intense peak at 1692 cm^{-1} were ascribed to the O–H stretching vibration and the C═O stretching vibration, respectively. The absorption band around 1618 cm^{-1}, 1534 cm^{-1}, and 1456 cm^{-1} was assigned to the aromatics ring. The spectrum of the α-Amy/SK@EGCG included all of the characteristic peaks of α-Amy and EGCG, proving the presence of both components. However, the broadening peaks of O–H shift from 3406 to 3340 cm^{-1} and the weakening of the amide I band peak at 1650 cm^{-1} indicates that the α-Amy/SK@EGCG emulsion was formed by the hydrogen bonding interaction between α-Amy and EGCG. Meanwhile, the C═O stretching vibration of EGCG shifts from 1692

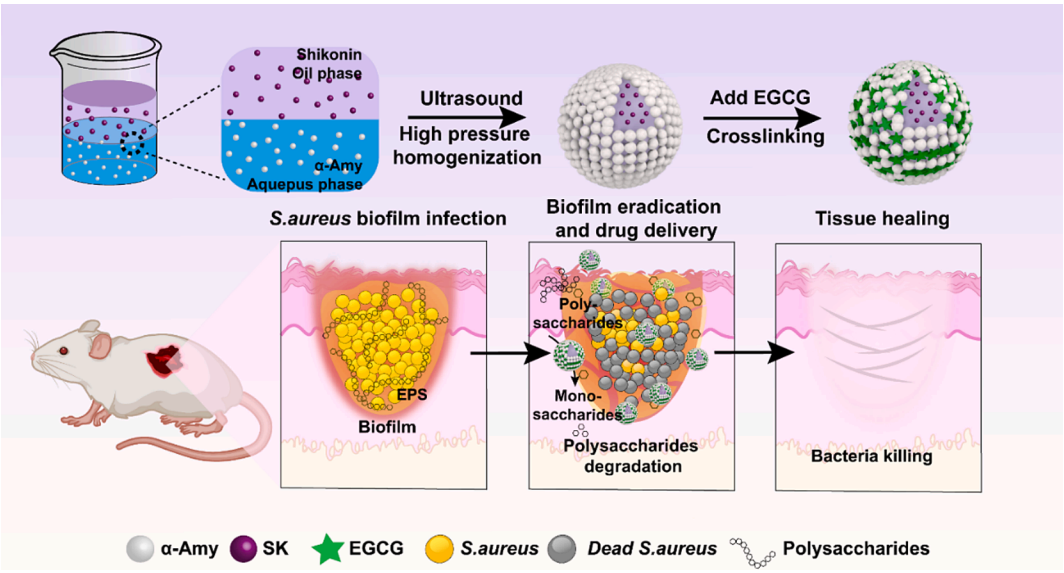

Scheme 1. The schematic diagram of the preparation process of α-Amy/SK@EGCG emulsion and the degradation of biofilms in wounds.

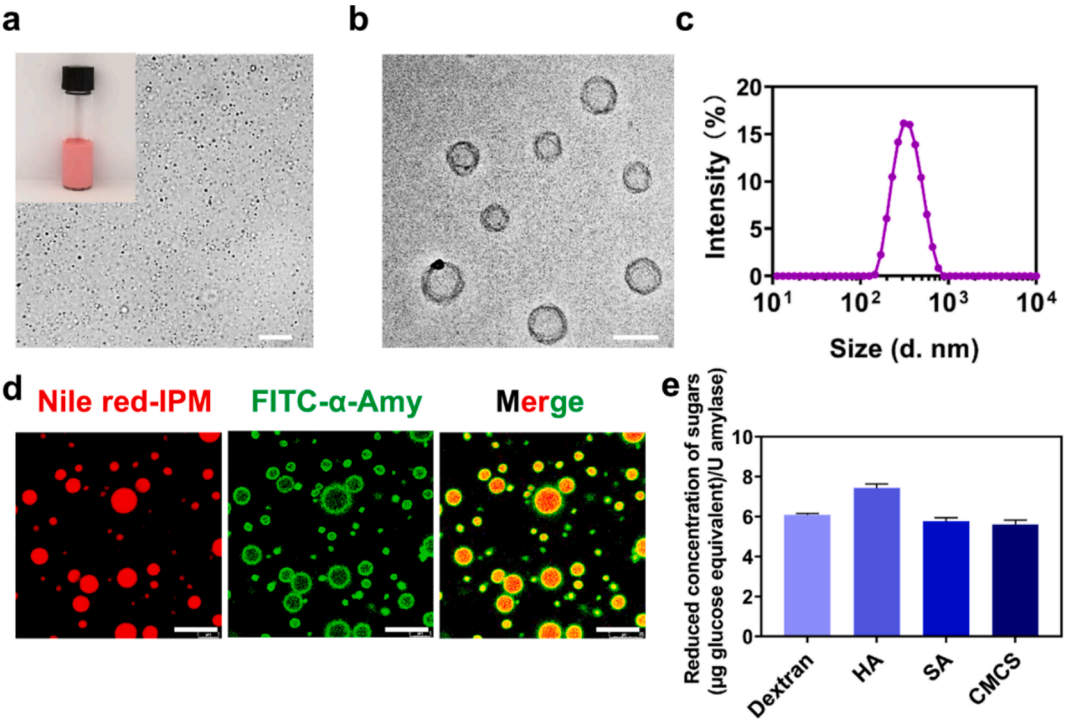

Fig. 1. (a) Optical microscopy of α-Amy/SK@EGCG emulsion and visual aspect of the emulsion (inset). Scale bar is 20 μm. (b) TEM image of α-Amy/SK@EGCG emulsion. Scale bar is 500 nm. (c) Hydrated diameter distribution profiles of α-Amy/SK@EGCG emulsion droplets measured in water. (d) CLSM images of Nile red-labeled IPM and FITC-labeled α-Amy in the emulsion. Scale bars are 10 μm. (e) Reducing sugar concentration after *in vitro* treatment of polysaccharides with the α-Amy/SK@EGCG emulsion.

cm^{-1} to 1688 cm^{-1}, which also indicates the crosslinking of α-Amy and EGCG. To further study the emulsion structure, large-sized emulsions were prepared by lowering the power of ultrasound. For this purpose, the aqueous and oil phases were dyed. From the CLSM images (Fig. 1d), it can be observed that the α-Amy protein (green) was distributed at the interface between the aqueous and oil phases, while IPM (red) was distributed inside the droplets, indicating that α-Amy was evenly distributed at the surface of the emulsion droplets. Furthermore, the stability of the emulsions was study by monitoring the changes in droplet size over a 7 day, The average droplet diameter increased slightly which is attributed to the Ostwald ripening. After the initial adjustment, the droplet size remained stable throughout the 7 day period (Fig. S5). This indicates that the emulsion system reached a dynamic equilibrium, and the interfacial film formed by α-amylase and EGCG through hydrogen bonding effectively prevented further coalescence or phase separation. As for effect of ultrasonic parameters on emulsion stability, phase separation and sedimentation were monitored visually and quantitatively after 5 day of storge. At low power (30–100 W) , phase separation occurred after 5 day of storge. (Fig. S3b), attributed to insufficient energy input to fully disrupt oil/water interfaces.

However, no phase separation or sedimentation was observed for the emulsions prepared at 150 W. At 150 W, the acoustic cavitation generated sufficient shear forces to break droplets into nanoscale sizes while maintaining emulsifier (α-Amy) integrity. Furthermore, the encapsulation efficiency of SK in the α-Amy/SK@EGCG emulsion was found to be 97 ± 0.57 % as determined by HPLC (Fig. S6). In this regard, it was observed that the hydrophobic SK was efficiently encapsulated in the O/W emulsion.

Considering the α-Amy enzyme is efficient in degrading polysaccharide into monosaccharide, the degradation ability of α-Amy/SK@EGCG emulsion into EPS in vitro was evaluated by a DNS (3,5-dinitrosalicylic acid) method. We investigated *in vitro* the ability of Amy/SK@EGCG emulsion to degrade several model exopolysaccharides including dextran, hyaluronic acid (HA), carboxymethyl chitosan (CMCS) and sodium alginate (SA) (Fig. 1e). The α-Amy/SK@EGCG emulsion effectively hydrolyzed the α-1,4-glucosidic bonds within HA, yielding a significant quantity of reducing sugar (7.4 ± 0.21 μg/U, equivalent to glucose). In contrast, the content of reducing sugar for dextran, CMCS and SA after treatment with the emulsion were 6.1 ± 0.06 μg/U, 5.6 ± 0.21 μg/U and 5.8 ± 0.18 μg/U, respectively, which were less pronounced than HA. These findings suggest that the α-Amy dispersed at the oil–water interface of α-Amy/SK@EGCG emulsion possess an enhanced degradation capability for the EPS mimics. Consequently, the bacteria in the biofilm could be easily exposed to antimicrobial agents, facilitating deeper penetration and more effective eradication of biofilm.

2.2. *In vitro anti-biofilm activity*

Based on the enhanced degradation ability to EPS mimics, the α-Amy/SK@EGCG emulsion was expected to have the potential of eradicating biofilms (Fig. 2a). The CLSM images showed that the *S. aureus* bacterial film reached a thickness of approximately 10 μm for the control group (PBS treatment) without any significant bacterial mortality (Fig. 2b). The group treated with CaS/SK@EGCG(casein sodium (CaS) as the control which does not possess enzymatic catalytic ability) also showed a relatively thick *S. aureus* biofilm (8 μm) and almost no bacterial death, which indicated that SK could not sufficiently penetrate the biofilm to kill the bacteria. Interestingly, the biofilm treated with the α-Amy@EGCG emulsion was disrupted and a significant amount of the bacteria died. This can be ascribed to the degradation ability of α-Amy to EPS matrix barrier, while the presence of EGCG contributes to its antibacterial ability, resulting in partial disruption of the biofilm. Compared with the above groups, the biofilm thickness was significantly reduced and a large number of bacteria died after treatment with α-Amy/SK@EGCG emulsion. The results confirmed that α-Amy played an indispensable role in degrading biofilms, while EGCG and SK could effectively penetrate into the matrix and synergistically achieve a remarkable antibacterial effect.

The inhibitory effect of the emulsions on *S. aureus* biofilm formation can be quantitatively assessed by crystal violet staining. As shown in Fig. 3a, the biofilm eradication efficacy of the emulsion was evaluated by measuring the biomass of biofilm with crystal violet staining methods. In this sense, the PBS group and CaS/SK@EGCG treated group were of the least affected, while the α-Amy/SK@EGCG treatment resulted in a significantly reduced color intensity, indicating a diminished biofilm formation. As shown in Fig. 3b, α-Amy/SK@EGCG emulsion treatment could significantly inhibit biofilm formation of *S. aureus* in comparison to the other three treatments, resulting in a 74 % reduction of biofilm formation when compared with the control treatment. Therefore, the α-Amy/SK@EGCG emulsion was effective in eradicating bacterial biofilm.

In order to further analyze the microstructural changes of biofilm after the treatment with Amy/SK@EGCG emulsion, a morphological analysis of the remaining biofilm was performed by SEM. In the PBS (control) group, the *S. aureus* accumulated to form a dense biofilm, which can be clearly seen in Fig. 3c. The morphology of the bacteria treated with α-Amy/SK@EGCG is significantly different from the PBS group, as the biofilms were almost completely dispersed in the SEM images. Besides, some bacteria ruptured and collapsed in the control

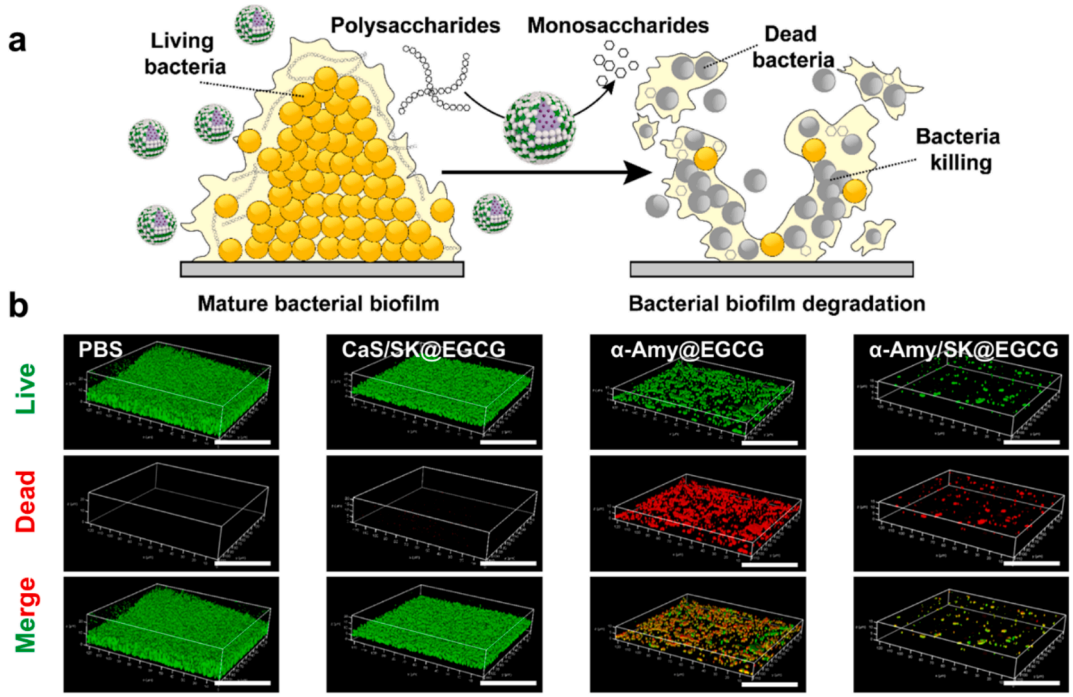

Fig. 2. (a) Schematic diagram for the degradation process of bacterial biofilm. α-Amylase catalyzes the conversion of polysaccharides within the extracellular matrix of bacterial biofilms into monosaccharides (glucose) to degrade EPS matrix barrier, thereby EGCG and SK could effectively penetrate into the matrix, inducing effectively eradicating bacteria. (b) CLSM images of biofilms treated with PBS, CaS/SK@EGCG, α-Amy@EGCG, or α-Amy/SK@EGCG emulsions, respectively. Scale bars are 50 μm.

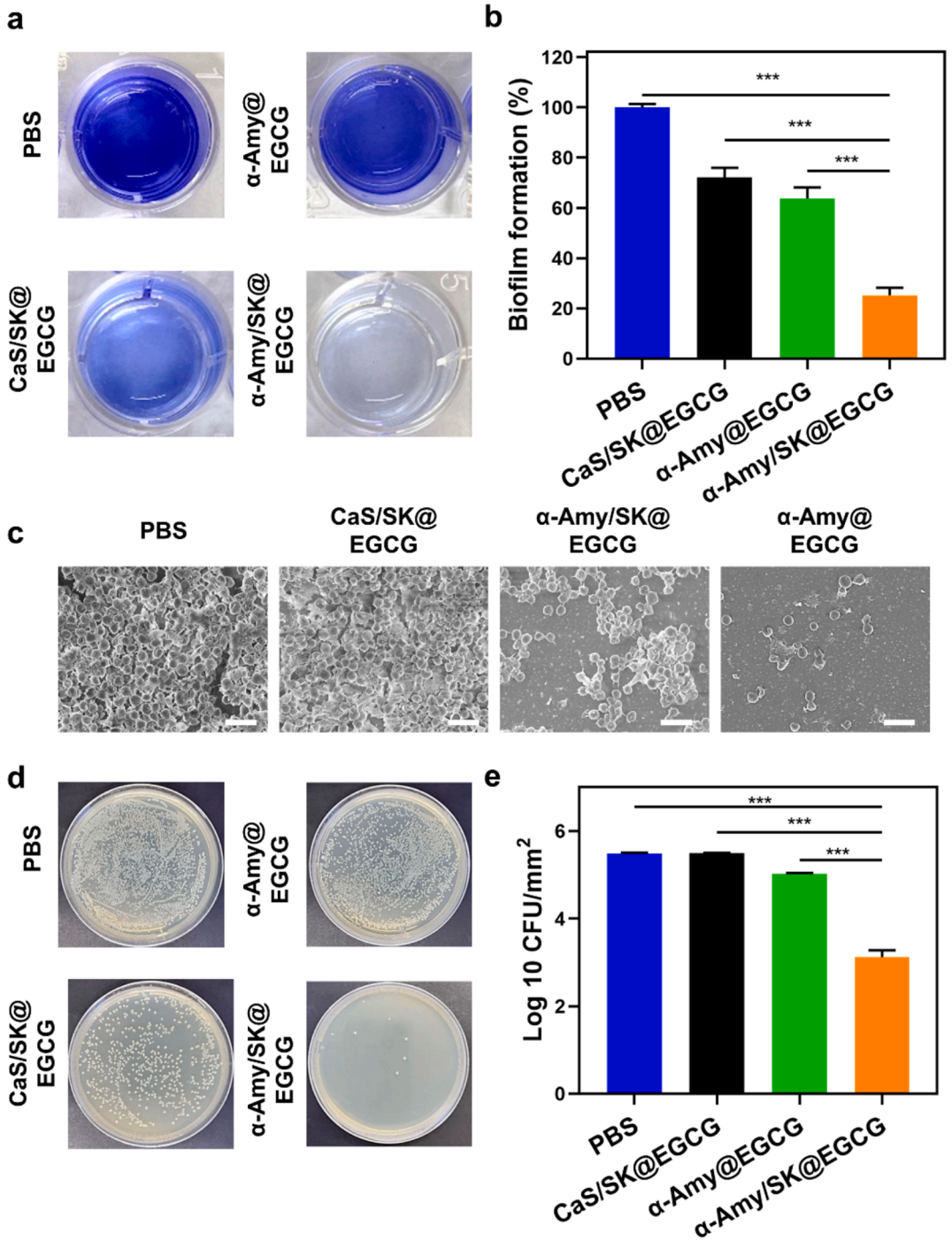

Fig. 3. (a) Images of crystal violet stained biofilms treated with PBS, CaS/SK@EGCG, α-Amy@EGCG or α-Amy/SK@EGCG emulsions, and the corresponding biofilm inhibition rate of each treatment group (b). (c) SEM images of *S. aureus* biofilms after treatment with PBS, CaS/SK@EGCG, α-Amy@EGCG or α-Amy/SK@EGCG emulsions, respectively (Scale bars are 2 μm). (d) Pictures of *S. aureus* colonies on agar plates after treatment with PBS, CaS/SK@EGCG, α-Amy@EGCG, or α-Amy/SK@EGCG emulsions, and the corresponding bacterial survival rate of each treatment group (e). Data are represented as mean ± SD (*$p < 0.05$, **$p < 0.01$, ***$p < 0.001$, p****<0.0001).

group, which also proves that α-Amy/SK@EGCG emulsion could effectively degrade the *S. aureus* biofilm.

While for the bactericidal performance, it can be observed that the treatment effectiveness of α-Amy@EGCG and α-Amy/SK@EGCG emulsions was higher than CaS/SK@EGCG emulsions (when compared with PBS group). Since there were almost no colonies observed after treatment, α-Amy/SK@EGCG is considered as the most effective for bacterial biofilm eradication (Fig. 3d). The bacterial growth rate of CaS/SK@EGCG (5.49 ± 0.012 CFU/mm^2) or α-Amy@EGCG (5.02 ± 0.024 CFU/mm^2) emulsions treated group only showed a slight drop in comparison with the PBS group (5.49 ± 0.018 CFU/mm^2, Fig. 3e). However, the α-Amy/SK@EGCG group showed significantly better bacteriostatic effect to *S. aureus* (bacterial growth rate of 3.12 ± 0.156 CFU/mm^2) due to the combined action of SK and EGCG. The α-Amy-catalyzed the degradation of EPS to make bacteria exposed, while SK and EGCG played a good antibacterial role.

2.3. In vivo anti-biofilm activity

In order to verify the biosafety of the α-Amy/SK@EGCG emulsion, cell viability was determined by co-incubation of NIH-3T3 cells with different concentrations of α-Amy (Fig. S7). Even when the cells were treated with emulsions containing 250 μg/mL of α-Amy, the survival rate of NIH-3T3 cells was still higher than 90 %. In this sense, the α-Amy/SK@EGCG emulsion did not cause significant cytotoxicity. To further investigate the *in vivo* anti-biofilm effect of the α-Amy/SK@EGCG emulsion, a biofilm-infected wound model was established using mice. As shown in Fig. 4a, the mice were randomly divided into four groups and treated with different emulsions every 2 days (PBS, CaS/SK@EGCG, α-Amy@EGCG or α-Amy/SK@EGCG). The wound healing process after each drug administration procedure was recorded by photography.

As shown in Fig. 4b, the mice treated with PBS showed severe pus formed on the wound until day 6. Similar occurrence of infection condition was observed for the group treated with the CaS/SK@EGCG emulsion, with abscess and scab being present until day 4. For both groups, the wounds were not completely healed on day 8. In the case of the CaS/SK@EGCG emulsion, because of the unbroken biofilm the healing time was prolonged, which prevents the in-depth contact of the antibacterial agents with the bacteria on the wound. Regarding the treatment with α-Amy@EGCG emulsions containing α-Amy, it can be seen that the wound healing process of the mice was greatly improved. The wound abscess after treatment with α-Amy@EGCG started to improve on day 2, and the wound area was significantly reduced on day 6 (Fig. 4c). In contrast, for the group treated with α-Amy/SK@EGCG emulsion, the addition of α-Amy significantly accelerated the healing rate of biofilm-infected wounds, and the wound was almost completely healed on day 8. The accelerated healing rate was due to the degradation of polysaccharide in the extracellular matrix of bacteria, which made the encapsulated bacteria exposed.

On day 8 of treatment, the skin surrounding the wound site of all the groups was taken for further histological analysis. From Fig. 4d obvious inflammation was observed in the wound site of the PBS group. The depressed skin around the wound site and the loosely arranged tissue of these controlled group, indicates that the wound would not heal completely without the combined utilization of α-Amy and SK. While for the α-Amy/SK@EGCG emulsion treated group, a mastoid layer on the

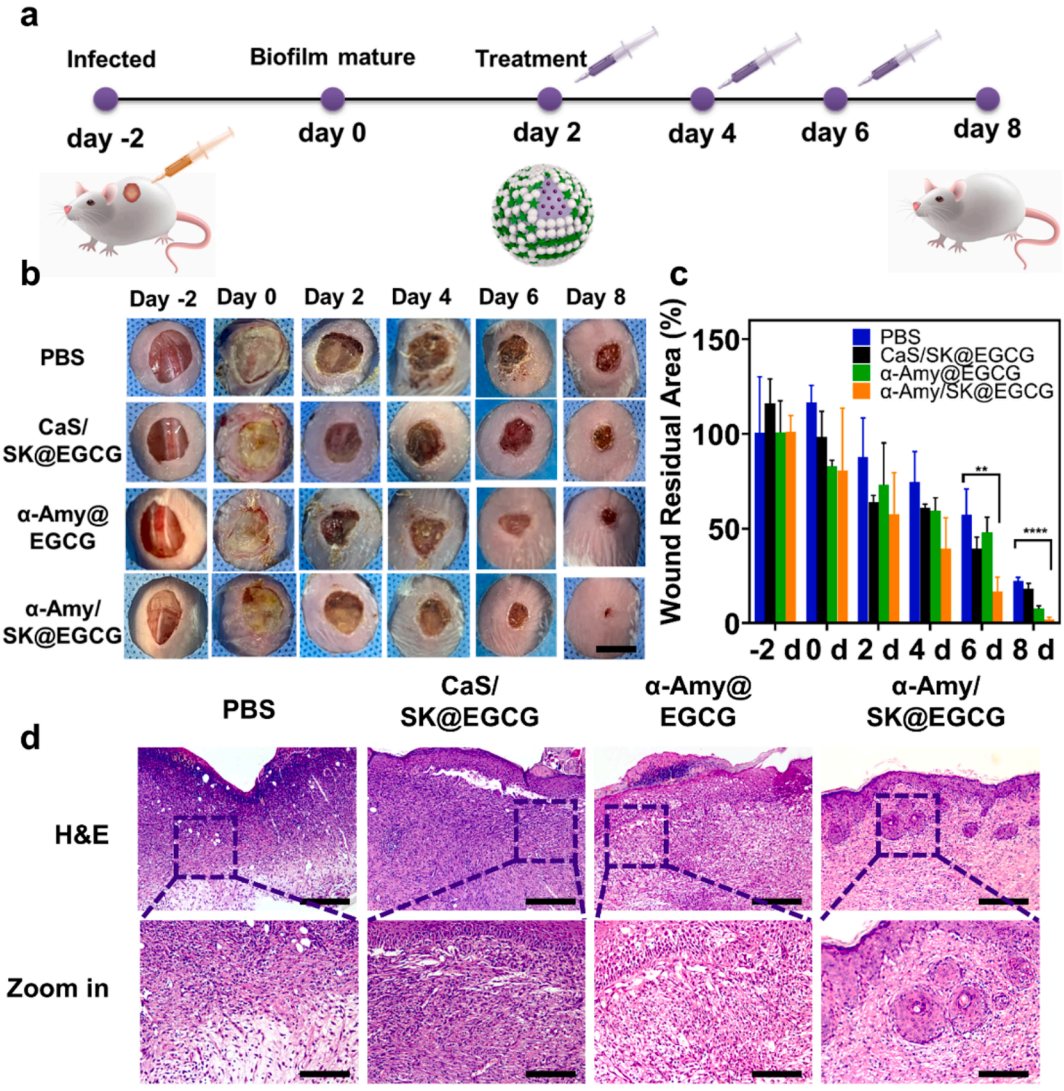

Fig. 4. (a) Schematic diagram for the biofilm infection and treatment of wound in mice. (b) Photographs of biofilm-infected wounds treated with PBS, CaS/SK@EGCG, α-Amy@EGCG or α-Amy/SK@EGCG emulsions at −2, 0, 2, 4, 6 and 8 days, respectively. Scale bars represent 1 mm. (c) Statistical histogram corresponding to wound area over 8 days of treatment with PBS, CaS/SK@EGCG, α-Amy@EGCG or α-Amy/SK@EGCG emulsions. Data are represented as mean ± standard deviation (*$p < 0.05$, **$p < 0.01$, ***$p < 0.001$, p****<0.0001). (d) Histological analysis using H&E staining on the wound tissue. Scale bars represent 200 μm (top) and 100 μm (bottom).

granulation tissue was appeared, demonstrating the complete healing of the wound. Both the results of wound test and histological analysis demonstrate the excellent bactericidal effects of α-Amy/SK@EGCG emulsion.

A *S. aureus* infected wound model was established to evaluate the antibacterial effect of the emulsion *in vivo* and the length of the wound was measured on day 8 (Fig. 5a). Among all the tested groups (Fig. 5b), the wound length of the group treated with α-Amy/SK@EGCG emulsion was the smallest (2.35 ± 0.42 mm). From the statistical analysis, it can be observed that treatments using the α-Amy@EGCG emulsions resulted in significantly shorter wound length (3.86 ± 0.21 mm) after 8 days. Especially, the α-Amy/SK@EGCG emulsion can effectively accelerated the healing of biofilm-infected wounds, which is evidenced by the significantly shorter wound length after 8 days when compared to the control group (5.86 ± 0.19 mm).

Collagen deposition during wound repair process serves as a key indicator for wound healing and skin repair. After Masson staining of mouse skin tissue, the deposition of collagen could be observed (Fig. 5c). For the group treated with α-Amy/SK@EGCG emulsion, an enhanced collagen accumulation was observed as largest blue area was observed which represents the collagen fiber content and distribution in the tissue. On the other hand, rare collagen deposition was observed for PBS, CaS/SK@EGCG and α-Amy@EGCG groups, which indicates an incomplete and postponed healing process of the wound. As shown in Fig. 5d, statistical analysis showed that the collagen volume fraction in the PBS, CaS/SK@EGCG, α-Amy@EGCG, and α-Amy/SK@EGCG groups were 24.9 ± 3.5 %, 34.7 ± 1.9 %, 53.7 ± 6.4 %, and 69.8 ± 3.9 %, respectively (Fig. 5d). The significant disparity of collagen deposition between the α-Amy/SK@EGCG emulsion and the other three groups suggests that the α-Amy/SK@EGCG emulsion could effectively reduce the inflammation response of wounds, which was consistent with the results of H&E staining. The pronounced effect of α-Amy/SK@EGCG emulsion is primarily ascribed to the anti-inflammatory effects of SK and EGCG, implying a potent anti-biofilm effect and accelerated wound healing.

Angiogenesis is another indicator of wound healing. The CD31 immunostaining of wound tissues were carried out and shown in Fig. 5e. New blood vessel formation was observed in the mice skin tissue after treatment with the α-Amy/SK@EGCG emulsion, correlating with complete wound closure. Subsequent H&E stained sections from the major organs of these treated mice further confirmed the biocompatibility of the α-Amy/SK@EGCG emulsion, which would not cause any systemic inflammatory response (Fig. S8). These findings made the α-Amy/SK@EGCG emulsion an excellent candidate for the management of wounds compromised by biofilm infections.

3. Conclusion

In conclusion, an innovative approach was introduced for the degradation of bacterial biofilm and acceleration of wound healing. The stable α-Amy/SK@EGCG emulsion was facilitated by using the amphiphilic α-Amy as stabilizer, coupled with the application of ultrasound assistance to encapsulate SK. The incorporation of EGCG served to enhance the emulsion stability through the crosslinking of proteins on the surfaces. The α-Amy at the O/W interface of this emulsion could efficiently degrade the EPS of *S. aureus* biofilm, thereby exposing the bacteria to enhance the permeability and efficient delivery of the natural hydrophobic antibacterial reagent (i.e., SK) to wound sites. Moreover, the utilization of EGCG and SK circumvented the requirement of synthetic antibiotics. The emulsions promoted the synergistic degradation of biofilms and the localized accumulation and transportation of specific drugs, thereby eradicating bacteria. The findings indicate that the α-Amy/SK@EGCG emulsion significantly advance the healing process of wounds infected with biofilms. This strategy offers a novel perspective for the development of materials capable of degrading the EPS of biofilms within the wound and promoting wound healing process.

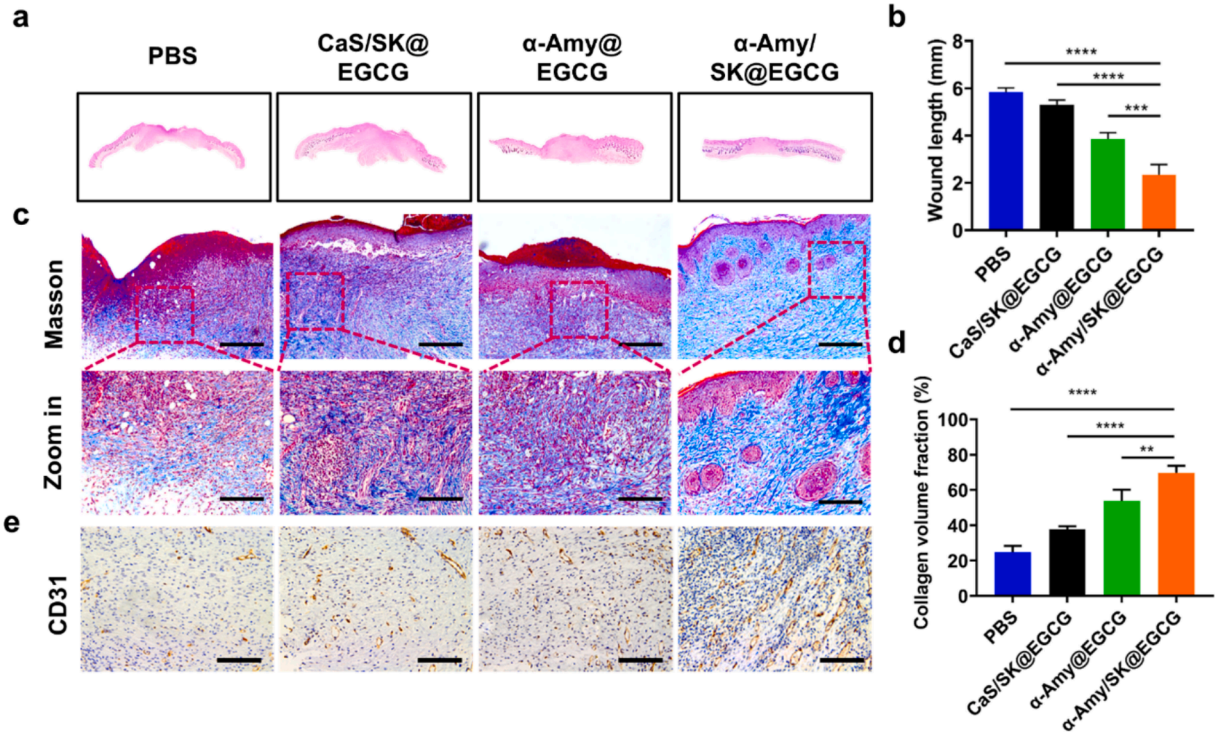

Fig. 5. Histological staining to analyze the healing of mice wound tissue after 8 days treatment with PBS, CaS/SK@EGCG, α-Amy@EGCG or α-Amy/SK@EGCG emulsions. (a) Panoramic photos using H&E staining. (b) Photographs of Masson staining analysis. Scale bars are 200 μm (top) and 100 μm (bottom). (c) CD31 immunostaining. Scale bars are 100 μm. (d) Histogram for statistical analysis of wound length. Data are represented as mean ± SD (*p < 0.05, **p < 0.01, ***p < 0.001, p****<0.0001). (e) Histogram for collagen deposition analysis of wound tissue. Data are represented as mean ± SD (*p < 0.05, **p < 0.01, ***p < 0.001, p****<0.0001).

CRediT authorship contribution statement

Xiaomiao Cui: Writing – review & editing, Writing – original draft, Methodology, Investigation, Formal analysis, Data curation. **Zhiliang Gao:** Methodology, Formal analysis, Conceptualization. **Xinxin Han:** Investigation, Formal analysis, Data curation. **Qun Yu:** Formal analysis, Data curation, Conceptualization. **Vitoria H. Cauduro:** Methodology, Conceptualization. **Erico M.M. Flores:** Visualization, Methodology, Conceptualization. **Muthupandian Ashokkumar:** Methodology, Formal analysis, Conceptualization. **Xiaoyong Qiu:** Writing – review & editing, Supervision, Formal analysis, Data curation, Conceptualization. **Jiwei Cui:** Writing – review & editing, Supervision, Resources, Funding acquisition, Formal analysis, Data curation, Conceptualization.

Declaration of competing interest

The authors declare that they have no known competing financial interests or personal relationships that could have appeared to influence the work reported in this paper.

Acknowledgements

This research was supported by the National Natural Science Foundation of China (22372091, 22202117), International Cooperation Project of Shandong Province (WST2021019), and the Center for International Cooperation and Disciplinary Innovation (B20033). This work was performed in part at the Analytical Centre for Structural Constituent and Physical Property.

Appendix A. Supplementary data

Supplementary data to this article can be found online at https://doi.org/10.1016/j.ultsonch.2025.107302.

References

[1] J.P. Motta, J.L. Wallace, A.G. Buret, C. Deraison, N. Vergnolle, Gastrointestinal biofilms in health and disease, Nat. Rev. Gastroenterol. Hepatol. 18 (2021) 314–334, https://doi.org/10.1038/s41575-020-00397-y.
[2] H.C. Flemming, J. Wingender, U. Szewzyk, P. Steinberg, S.A. Rice, S. Kjelleberg, Biofilms: an emergent form of bacterial life, Nat. Rev. Microbiol. 14 (2016) 563–575, https://doi.org/10.1038/nrmicro.2016.94.
[3] O. Ciofu, C. Moser, P.O. Jensen, N. Hoiby, Tolerance and resistance of microbial biofilms, Nat. Rev. Microbiol. 20 (2022) 621–635, https://doi.org/10.1038/s41579-022-00682-4.
[4] Y. Su, J.T. Yrastorza, M. Matis, J. Cusick, S. Zhao, G. Wang, J. Xie, Biofilms: formation, research models, potential targets, and methods for prevention and treatment, Adv. Sci. 9 (2022) e2203291, https://doi.org/10.1002/advs.202203291.
[5] S. Darvishi, S. Tavakoli, M. Kharaziha, H.H. Girault, C.F. Kaminski, I. Mela, Advances in the sensing and treatment of wound biofilms, Angew. Chem. Int. Ed. 61 (2022) e202112218, https://doi.org/10.1002/anie.202112218.
[6] L. Su, Y. Li, S. Tian, F. Huang, Y. Ren, C. Yang, H.C. van der Mei, H.J. Busscher, L. Shi, Synergy between pH- and hypoxia-responsiveness in antibiotic-loaded micelles for eradicating mature, infectious biofilms, Acta Biomater. 154 (2022) 559–571, https://doi.org/10.1016/j.actbio.2022.10.020.
[7] J. Xu, R. Danehy, H. Cai, Z. Ao, M. Pu, A. Nusawardhana, D. Rowe-Magnus, F. Guo, Microneedle patch-mediated treatment of bacterial biofilms, ACS Appl. Mater. Interfaces 11 (2019) 14640–14646, https://doi.org/10.1021/acsami.9b02578.
[8] Q. Yu, T. Deng, F.C. Lin, B. Zhang, J.I. Zink, Supramolecular assemblies of heterogeneous mesoporous silica nanoparticles to co-deliver antimicrobial peptides and antibiotics for synergistic eradication of pathogenic biofilms, ACS Nano 14 (2020) 5926–5937, https://doi.org/10.1021/acsnano.0c01336.
[9] H. Koo, R.N. Allan, R.P. Howlin, P. Stoodley, L. Hall-Stoodley, Targeting microbial biofilms: current and prospective therapeutic strategies, Nat. Rev. Microbiol. 15 (2017) 740–755, https://doi.org/10.1038/nrmicro.2017.99.
[10] E. Maslova, L. Eisaiankhongi, F. Sjoberg, R.R. McCarthy, Burns and biofilms: priority pathogens and *in vivo* models, NPJ Biofilms Microbiomes 7 (2021) 73, https://doi.org/10.1038/s41522-021-00243-2.
[11] D.S.W. Benoit, K.R. Sims Jr., D. Fraser, Nanoparticles for oral biofilm treatments, ACS Nano 13 (2019) 4869–4875, https://doi.org/10.1021/acsnano.9b02816.
[12] D.N. Huang, J. Wang, K.F. Ren, J. Ji, Functionalized biomaterials to combat biofilms, Biomater. Sci. 8 (2020) 4052–4066, https://doi.org/10.1039/d0bm00526f.
[13] Y. Xie, K. Qiao, L. Yue, T. Tang, Y. Zheng, S. Zhu, H. Yang, Z. Fang, A self-crosslinking, double-functional group modified bacterial cellulose gel used for antibacterial and healing of infected wound, Bioact. Mater. 17 (2022) 248–260, https://doi.org/10.1016/j.bioactmat.2022.01.018.
[14] P.C. Naha, Y. Liu, G. Hwang, Y. Huang, S. Gubara, V. Jonnakuti, A. Simon-Soro, D. Kim, L. Gao, H. Koo, D.P. Cormode, Dextran-coated iron oxide nanoparticles as biomimetic catalysts for localized and ph-activated biofilm disruption, ACS Nano 13 (2019) 4960–4971, https://doi.org/10.1021/acsnano.8b08702.
[15] M. Liang, Y. Wang, K. Ma, S. Yu, Y. Chen, Z. Deng, Y. Liu, F. Wang, Engineering inorganic nanoflares with elaborate enzymatic specificity and efficiency for versatile biofilm eradication, Small 16 (2020) e2002348, https://doi.org/10.1002/smll.202002348.
[16] S. Obuobi, A. Ngoc Phung, K. Julin, M. Johannessen, N. Skalko-Basnet, Biofilm responsive zwitterionic antimicrobial nanoparticles to treat cutaneous infection, Biomacromolecules 23 (2022) 303–315, https://doi.org/10.1021/acs.biomac.1c01274.
[17] S. Wu, C. Xu, Y. Zhu, L. Zheng, L. Zhang, Y. Hu, B. Yu, Y. Wang, F.J. Xu, Biofilm-sensitive photodynamic nanoparticles for enhanced penetration and antibacterial efficiency, Adv. Funct. Mater. 31 (2021) 2103591, https://doi.org/10.1002/adfm.202103591.
[18] D. Hu, L. Zou, W. Yu, F. Jia, H. Han, K. Yao, Q. Jin, J. Ji, Relief of biofilm hypoxia using an oxygen nanocarrier: a new paradigm for enhanced antibiotic therapy, Adv. Sci. 7 (2020) 2000398, https://doi.org/10.1002/advs.202000398.
[19] M. Ding, W. Zhao, X. Zhang, L. Song, S. Luan, Charge-switchable MOF nanocomplex for enhanced biofilm penetration and eradication, J. Hazard. Mater. 439 (2022) 129594, https://doi.org/10.1016/j.jhazmat.2022.129594.
[20] L. Tan, J. Li, X. Liu, Z. Cui, X. Yang, S. Zhu, Z. Li, X. Yuan, Y. Zheng, K.W.K. Yeung, H. Pan, X. Wang, S. Wu, Rapid biofilm eradication on bone implants using red phosphorus and near-infrared light, Adv. Mater. 30 (2018) e1801808, https://doi.org/10.1002/adma.201801808.
[21] J. Wang, L. Wang, J. Pan, J. Zhao, J. Tang, D. Jiang, P. Hu, W. Jia, J. Shi, Magneto-based synergetic therapy for implant-associated infections *via* biofilm disruption and innate immunity regulation, Adv. Sci. 8 (2021) 2004010, https://doi.org/10.1002/advs.202004010.
[22] N. Gurung, S. Ray, S. Bose, V. Rai, A broader view: microbial enzymes and their relevance in industries, medicine, and beyond, Biomed Res. Int. 2013 (2013) 329121, https://doi.org/10.1155/2013/329121.
[23] H.C. Moon, S. Han, J. Borges, T. Pesqueira, H. Choi, S.Y. Han, H. Cho, J.H. Park, J. F. Mano, I.S. Choi, Enzymatically degradable, starch-based layer-by-layer films: application to cytocompatible single-cell nanoencapsulation, Soft Matter 16 (2020) 6063–6071, https://doi.org/10.1039/d0sm00876a.
[24] A. Ivanova, K. Ivanova, I. Perelshtein, A. Gedanken, K. Todorova, R. Milcheva, P. Dimitrov, T. Popova, T. Tzanov, Sonochemically engineered nano-enabled zinc oxide/amylase coatings prevent the occurrence of catheter-associated urinary tract infections, Mater. Sci. Eng. C Mater. Biol. Appl. 131 (2021) 112518, https://doi.org/10.1016/j.msec.2021.112518.
[25] K. Ivanova, M.M. Fernandes, A. Francesko, E. Mendoza, J. Guezguez, M. Burnet, T. Tzanov, Quorum-quenching and matrix-degrading enzymes in multilayer coatings synergistically prevent bacterial biofilm formation on urinary catheters, ACS Appl. Mater. Interfaces 7 (2015) 27066–27077, https://doi.org/10.1021/acsami.5b09489.
[26] J. Xie, Z. Meng, X. Han, S. Li, X. Ma, X. Chen, Y. Liang, X. Deng, K. Xia, Y. Zhang, H. Zhu, T. Fu, Cholesterol microdomain enhances the biofilm eradication of antibiotic liposomes, Adv. Healthc. Mater. 11 (2022) e2101745, https://doi.org/10.1002/adhm.202101745.
[27] S.E. Birk, J.A.J. Haagensen, H.K. Johansen, S. Molin, L.H. Nielsen, A. Boisen, Microcontainer Delivery of Antibiotic Improves Treatment ofPseudomonas aeruginosa Biofilms, Adv. Healthc. Mater. 9 (2020) e1901779, https://doi.org/10.1002/adhm.201901779.
[28] H. Le, C. Arnoult, E. De, D. Schapman, L. Galas, D. Le Cerf, C. Karakasyan, Antibody-conjugated nanocarriers for targeted antibiotic delivery: application in the treatment of bacterial biofilms, Biomacromolecules 22 (2021) 1639–1653, https://doi.org/10.1021/acs.biomac.1c00082.
[29] Q. Jing, H. Ruan, J. Li, Z. Wang, L. Pei, H. Hu, Z. He, T. Wu, S. Ruan, T. Guo, Y. Wang, N. Feng, Y. Zhang, Keratinocyte membrane-mediated nanodelivery system with dissolving microneedles for targeted therapy of skin diseases, Biomaterials 278 (2021) 121142, https://doi.org/10.1016/j.biomaterials.2021.121142.
[30] Q. Sun, T. Gong, M. Liu, S. Ren, H. Yang, S. Zeng, H. Zhao, L. Chen, T. Ming, X. Meng, H. Xu, Shikonin, a naphthalene ingredient: Therapeutic actions, pharmacokinetics, toxicology, clinical trials and pharmaceutical researches, Phytomedicine 94 (2022) 153805, https://doi.org/10.1016/j.phymed.2021.153805.
[31] X. Ning, C. Wiraja, W.T.S. Chew, C. Fan, C. Xu, Transdermal delivery of Chinese herbal medicine extract using dissolvable microneedles for hypertrophic scar treatment, Acta Pharm. Sin. B 11 (2021) 2937–2944, https://doi.org/10.1016/j.apsb:2021.03.016.
[32] G. Shu, D. Xu, W. Zhang, X. Zhao, H. Li, F. Xu, L. Yin, X. Peng, H. Fu, L.J. Chang, X. R. Yan, J. Lin, Preparation of shikonin liposome and evaluation of its *in vitro* antibacterial and *in vivo* infected wound healing activity, Phytomedicine 99 (2022) 154035, https://doi.org/10.1016/j.phymed.2022.154035.
[33] Y. Chevalier, M.-A. Bolzinger, Emulsions stabilized with solid nanoparticles: Pickering emulsions, Colloid Surf. A 439 (2013) 23–34, https://doi.org/10.1016/j.colsurfa.2013.02.054.
[34] X. Zhang, H. Geng, C. Shan, X. Cui, X. Zhang, M. Ashokkumar, J. Cui, P. Zhang, Assembly of emulsion-based cascade vehicles for combination

oxygen–chemotherapy in diabetic wound healing, Langmuir 40 (2024) 19766–19774, https://doi.org/10.1021/acs.langmuir.4c02549.
[35] M. Zhang, Q. Cao, Y. Yuan, X. Guo, D. Pan, R. Xie, X. Ju, Z. Liu, W. Wang, L. Chu, Functional nanoemulsions: Controllable low-energy nanoemulsification and advanced biomedical application, Chin. Chem. Lett. 35 (2024) 108710, https://doi.org/10.1016/j.cclet.2023.108710.
[36] S. Hiranphinyophat, A. Otaka, Y. Asaumi, S. Fujii, Y. Iwasaki, Particle-stabilized oil-in-water emulsions as a platform for topical lipophilic drug delivery, Colloid Surf. B 197 (2021) 111423, https://doi.org/10.1016/j.colsurfb.2020.111423.
[37] V. Andretto, G. Taurino, G. Guerriero, H. Guerin, E. Laine, M.G. Bianchi, G. Agusti, S. Briancon, O. Bussolati, A. Clayer-Montembault, G. Lollo, Nanoemulsions embedded in alginate beads as bioadhesive nanocomposites for intestinal delivery of the anti-inflammatory drug tofacitinib, Biomacromolecules 24 (2023) 2892–2907, https://doi.org/10.1021/acs.biomac.3c00260.
[38] H.B. Jadhav, P. Choudhary, P. Gogate, S. Ramniwas, R. Mugabi, Z. Ahmad, S. Mohammed Basheeruddin Asdaq, G. Ahmad Nayik, Sonication as a potential tool in the formation of protein-based stable emulsion: concise review, Ultrason. Sonochem. 107 (2024) 106900, https://doi.org/10.1016/j.ultsonch.2024.106900.
[39] X. Cui, Z. Gao, K. Zhao, N. Wang, Q. Yu, M. Ashokkumar, J. Hao, J. Cui, Sono-assembly of polyphenol–protein capsules for enhanced biocatalytic cascades, Chem. Mater. 36 (2024) 8864–8871, https://doi.org/10.1021/acs.chemmater.4c01698.
[40] N. Zainuddin, I. Ahmad, M.H. Zulfakar, H. Kargarzadeh, S. Ramli, Cetyltrimethylammonium bromide-nanocrystalline cellulose (CTAB-NCC) based microemulsions for enhancement of topical delivery of curcumin, Carbohydr. Polym. 254 (2021) 117401, https://doi.org/10.1016/j.carbpol.2020.117401.
[41] T. Zhang, J. Xu, J. Chen, Z. Wang, X. Wang, J. Zhong, Protein nanoparticles for Pickering emulsions: A comprehensive review on their shapes, preparation methods, and modification methods, Trends Food Sci. Technol. 113 (2021) 26–41, https://doi.org/10.1016/j.tifs.2021.04.054.
[42] A. Taha, E. Ahmed, A. Ismaiel, M. Ashokkumar, X. Xu, S. Pan, H. Hu, Ultrasonic emulsification: An overview on the preparation of different emulsifiers-stabilized Emulsions, Trends in Food Sci. Tech. 105 (2020) 363–377, https://doi.org/10.1016/j.tifs.2020.09.024.
[43] W. Lang, D. Mondol, A. Trakooncharoenvit, T. Tagami, M. Okuyama, T. Hira, N. Sakairi, A. Kimura, Formulation and evaluation of a novel megalomeric microemulsion from tamarind seed xyloglucan-megalosaccharides for improved high-dose quercetin delivery, Food Hydrocoll. 137 (2023) 108430, https://doi.org/10.1016/j.foodhyd.2022.108430.
[44] B. Lu, Y. Bo, M. Yi, Z. Wang, J. Zhang, Z. Zhu, Y. Zhao, J. Zhang, Enhancing the solubility and transdermal delivery of drugs using ionic liquid-in-oil microemulsions, Adv. Funct. Mater. 31 (2021) 2102794, https://doi.org/10.1002/adfm.202102794.